HHS Public Access

Author manuscript

Nat Commun. Author manuscript; available in PMC 2015 May 19.

Published in final edited form as:

Nat Commun. ; 5: 5499. doi:10.1038/ncomms6499.

Evolutionary triage governs fitness in driver and passenger mutations and suggests targeting never mutations

R A. Gatenby[1], **J. J. Cunningham**[1], and **J. S. Brown**[2]

[1]Cancer Biology and Evolution Program, Moffitt Cancer Center, Tampa. FL. 33612

[2]Department of Biological Sciences, University of Illinois at Chicago, Chicago, IL 60607

Abstract

Genetic and epigenetic changes in cancer cells are typically divided into “drivers” and “passengers”. Drug development strategies target driver mutations, but inter- and intra-tumoral heterogeneity usually results in emergence of resistance. Here we model intratumoral evolution in the context of a fecundity/survivorship trade-off. Simulations demonstrate the fitness value, of any genetic change is not fixed but dependent on evolutionary triage governed by initial cell properties, current selection forces, and prior genotypic/phenotypic trajectories. We demonstrate spatial variations in molecular properties of tumor cells are the result of changes in environmental selection forces such as blood flow. Simulated therapies targeting fitness-increasing (driver) mutations usually decrease the tumor burden but almost inevitably fail due to population heterogeneity. An alternative strategy targets gene mutations that are *never* observed. Because up or down regulation of these genes unconditionally reduces cellular fitness, they are eliminated by evolutionary triage but can be exploited for targeted therapy.

Introduction

The transition from normal to malignant phenotype during carcinogenesis, often described as “somatic evolution,” is associated with the accumulation of genetic (and epigenetic) mutations (1–4) but typically demonstrates convergence to common phenotypic properties (the cancer “hallmarks”(5)). Mutations are commonly characterized as a “driver” or “passenger” depending on contributions to proliferation and invasion (6,7). Targeted therapies can produce significant tumor response by disrupting driver mutations. However, not all tumors have identifiable and/or drugable driver mutations and response to targeted therapy, even when the driver mutation is present, is usually transient as resistant phenotypes repopulate the tumor (8).

Corresponding Author: Robert Gatenby, Moffitt Cancer Center, 12902 Magnolia Dr, Tampa, FL 33612, Phone: (813) 745-2834, Robert.Gatenby@Moffitt.org.

Author contributions

Designed study: RG, JC, JB. Performed computational experiments: JC. Wrote manuscript: RG, JC, JB.

Competing Financial Interests

The authors declare no competing financial interests

Here we investigate genetic heterogeneity, phenotypic convergence, the conventional binary classification of driver/passenger mutations and corresponding targeted therapy in the context of Darwinian dynamics. This extends ongoing efforts to understand cancer from first principles based on evolution by natural selection (9–11) including the classical trade-offs observed in Darwinian systems. Here, we consider a multi-loci diallelic model of mutation and selection within a finite population of tumor cells evolving along a well-defined adaptive landscape.

In examining the evolutionary dynamics during carcinogenesis, we assume that normal epithelial cells exist in an evolutionary and ecological state well below their maximal carrying capacity and individual evolutionary potential for survival and proliferation. That is, normal cells carry out their differentiated tasks for maintaining whole organism function and their population density, survival and proliferation is entirely controlled by tissue signals. Ecologically, a new cancer cell lineage begins with abundant available space (the lumen of a duct, for example) and is initially free from the life history trade-off of proliferation versus survivorship. Evolutionarily, the tumor lineage develops a self-defined fitness function, and then uses the human genome to evolve strategies to enhance survival and/or proliferation. Consistent with the fundamental laws of evolution, each population may initially undergo exponential proliferation but is ultimately ecologically constrained by limitations of substrate and space. Here, the evolutionary trajectory reaches the classical Darwinian life history tradeoff (12,13) in which cancer cells must invest limited available resources in some combination of survival and fecundity that maximizes fitness within the context of their environment. These phenotypic strategies are apparent in the consistent convergence to the “hallmarks” of cancer.

We use *in silico* simulations based on Darwinian first principles and classical evolutionary trade-offs to investigate the genomic dynamics that are both a cause and consequence of tumor development and progression. Our specific interests focus on the conventional designation of driver and passenger mutations, the source of observed spatial intratumoral heterogeneity, and the dynamics of tumor response and resistance to targeted therapies.

Our results demonstrate that the fitness value of most genetic and epigenetic events are contextual and depend on extant environmental selection forces, other local populations, and the prior evolutionary arc of the cell – dynamics that we collectively describe as “evolutionary triage.” We find that, as a result of evolutionary triage, the same mutation can act as passenger or driver depending on context. In a stable microenvironment, evolutionary triage will reduce tumor cell diversity so that the observed intratumoral molecular heterogeneity is due largely to variations in local selection pressures cause by, for example, blood flow. Our results demonstrate a previously unrecognized therapeutic target – “never” mutations. That is, when a gene is never or rarely observed to be mutated, we must conclude that up or down regulation that gene must unconditionally reduce cell fitness. We demonstrate that targeting never genes can be a highly effective therapeutic strategy.

Results

Evolutionary triage

Pooling genetic data from the 225 carcinogenesis simulations, we observed 3334 unique genotypes (5.09% of all possible genotypes) within the evolving cancers. Although the model randomly imposed mutations on each gene, the frequency with which each mutation was observable in the tumor was strongly influenced by its associated fitness change – a phenomenon we term “evolutionary triage.”

The observed frequency of neutral mutations is 0.6% per generation and at least one neutral mutation is found in ~25% of the cells in the final tumor populations. Thus, the observed frequency of passenger mutations per generation permits, as expected, a reasonable estimate of the actual mutation rate (which was 1% in our simulations). In some simulations, a neutral allele “hitchhiked” with a successful mutation and formed temporary linkage disequilibrium (Figures 1 and 2) so that it was present in a frequency greater than expected.

In Figure 1, we demonstrate the fitness advantage gained by mutations (green) conferring an increase in fecundity and/or survival allowed the cells with these mutations to proliferate more frequently. Consistent with clinical observations, driver genes are observed with far higher frequency (up to 92%) in the final tumor populations although with considerable variability.

Finally, mutations in genes (red) that resulted in a decrease of survival and or fecundity were observed during all of our simulations but became extinct quickly due to the fitness disadvantage. Their frequency in the final tumor was invariably near or equal to 0.

The basal cancer mutation rate

This study primarily examines the effects of evolutionary triage variations on the observed mutation rate in each gene. However, in identifying a basal mutation rate (Figure 2) we gained the unexpected insight that cancer evolution requires a “goldilocks” mutation rate. Specifically, a mutation rate that is too low (less than 10^{-3}) will not allow adequate exploration of the adaptive landscape and will result in a small, homogeneous and effectively “benign” tumor. On the other hand, a mutation rate that is too high (greater than 0.1) produces a mutation-selection balance in which fitness-reducing mutations occur too rapidly to be eliminated resulting in an overall decline in fitness and failure to reach the ESS. These dynamics could potentially be exploited for cancer prevention or treatment although this is beyond the current scope of the manuscript.

Intra-tumoral molecular heterogeneity

In Figure 3, we quantified tumor heterogeneity over time using the Simpson’s Index of Diversity (SID) which gives the probability that two randomly chosen tumor cells have different genotypes. A value close to 0 indicates very little genetic variability and a value of 1 indicates all individuals have a unique genotype.

We used the SID as virtual data in an Analysis of Variance between groups (ANOVA) with starting point (3 initial conditions), endpoint (ESS1, ESS2, ESS2 via ESS1, and intra-

tumoral areas of ESS1 and ESS2), and generation (35, 60, 100 and 1000) as independent variables. The analyses were performed in Systat (12) (see Supplementary Table 1). Our virtual patients were nested within the starting point by endpoint combinations, and we examined the three 2-way interactions between independent variables. All main effects and interaction effects were significant. This statistical model demonstrates about 60% (r^2=0.588) of the variation between patients can reflects variations in the properties of the adaptive landscape. However, patients frequently differed significantly from each other independent of the starting conditions or ending ESS ($F_{288,882}$=1.65, p<0.001), suggesting that early mutations and evolutionary trajectories remained persistent within a given patient over time.

Figure 3a demonstrates increased genetic variability occurs consistently early in carcinogenesis because the initial population grows with little inter- or intra-specific competition ($F_{3,882}$=19.10, p<0.001). That is, as the early populations expand into unoccupied space (the lumen of a duct or colon, for example) any genotype conferring higher fitness than the original normal population will proliferate. This first phase ends when the proliferation becomes limited by space and substrate and the tumor population evolves along the fecundity-survival tradeoff boundary. As shown in Figure 3, these Darwinian forces selects for the relatively small number of genotypes that confer maximal fitness and the population becomes more homogeneous as a small number of genotype-specific populations dominate. Furthermore, there is strong selection against any new genotype because no available strategy is fitter than the extant population. Thus, when tumor populations reach a fitness maximum, the *observed* mutation rate becomes effectively 0.

In contrast, tumors with spatially varying landscapes (in which, for example, ESS1 and ESS2 [Figure 3a] exist within the same tumor) or temporally varying landscapes (in which the entire tumor transitions from ESS1 to ESS2 [Figures 3c,3d]) maintain increased molecular heterogeneity when compared to a single, stable ESS environment ($F_{3,288}$=105.6, p<0.001). These results suggest that the observed molecular heterogeneity within tumors, rather than an unpredictable manifestation of random mutations, is dependent on variations in environmental selection forces, such as blood flow, and could be observed and predicted by clinical imaging (13).

Drivers, passengers, and never mutations

Driver mutations are defined as those that confer a proliferative advantage and are causally implicated in carcinogenesis (14). However, the simulation results demonstrate that identifying true driver mutations from an observed data set is difficult. Figure 4 shows data from “virtual biopsies” of 25 patient tumors for 12 possible evolutionary trajectories from normal to cancer. While a mutation in every gene is detectable in at least one patient “biopsy”, with the exception of gene 1, many of the mutations only occur in a minority of the cohort so that only 2 to 4 potential drivers are observed in ≥ 50% of the simulated patients within each group. These findings are consistent with observations of “hotspots” in the cancer genome in which there is apparently an increased mutation rate (15).

Thus, in each case, frequently observed mutations represent drivers that increase fitness and are causal in the transition of that cell from normal to cancer. However, in every cohort and

in every tumor some tumor cells achieved a maximally fit phenotype through less common combinations that reflect different genetic trajectories generated by chance or by environmental variations. For example, the mutation combination of [8, 11] confer virtually the same overall change in fecundity and survivorship as the mutation combination of [10, 16]. In tumors from initial phenotype 1 to ESS1, mutations 8 and 11 might be incorrectly viewed as of limited importance because they are relatively infrequently expressed.

These results are consistent with previously recognized limitations in identification of driver mutations from clinical data sets. However, our model results also demonstrate that conventional definitions of driver mutations should include an evolutionary and ecological context. Specifically, we find that the fitness value of any mutation qualitatively and quantitatively varies depending on:

1. the initial normal phenotype; Mutations in gene 4, which is a “driver” for cells originating from initial phenotype 3, are deleterious or “passenger mutations” for cells originating from phenotype 1.
2. The local environment both present and past; Evolution from phenotype 2 towards ESS1 selects for mutations in genes 4 and 7, while evolution from the same initial phenotype towards ESS2 selects for 3, 7, 8, 10, and 16. Gene 16 is strongly selected when initial phenotype 2 evolves to ESS2 but is rarely seen in tumors that first evolved to ESS1 and then transitioned to ESS2.
3. Prior mutational history. From initial phenotype 1 to ESS2, mutations in genes 15 and 16 confer the greatest fitness advantage. However, if a mutation in gene 8 first occurs, genes 15 and 16 become deleterious mutations and are not observed. (Supplementary Figure 1).

Evolutionary triage and targeted therapy

Figures 5 and 6 present simulation results from targeted therapy. In figure 5, therapy targets gene 16 which is the most commonly mutated gene in all evolutionary trajectories (Figure 4). For example, in simulations of 75 patient tumors evolved from each start point to ESS1, a complete and prolonged reduction in tumor burden was achieved in 9%. In 56.0% of patients targeted therapy achieves a significant response followed by adaptation and proliferation of resistant populations. In 28.0%, no reduction in tumor volume is observed although size stabilization with some delay in progression was observed in 7%. Resistance in our model occurs when cancer cell lineages that evolved without the target gene (often sparsely represented in the initial population) gain an adaptive advantage due to suppression of the dominant population and proliferate rapidly. Because of supervenience (16), alternative gene combinations replace and then evolve to maximize fitness.

These results for targeted therapy are consistent with clinical observations and conventional explanations for the results (17, 18). Does evolutionary triage suggest an alternative treatment strategy? Recall that, as a result of evolutionary triage, mutations that confer a decrease in fitness are virtually never observed in advanced cancers. We hypothesized that these genes might represent potential therapeutic targets. In our simulation gene 1 confers a negative change in both survivorship and proliferation. As a result, gene 1 would never be

considered a potential therapeutic target. Figure 6 shows the effect of a therapy that effectively up-regulates gene 1 in a tumor population originating from initial phenotype 1 to ESS1. We see that the forced upregulation of this gene can push tumor population fitness below 0 from ESS1 and results in complete extinction of the tumor population. The success of therapy demonstrates that, for "never gene" targets, every tumor cell is susceptible. Thus, although the simulations do not demonstrate complete extinction in every case (because some of the diverse tumor genotypes can overcome the negative fitness effects), all tumor were significantly affected.

Interestingly, combinations of therapy targeting driver and "never" mutations were consistently successful in causing complete tumor eradication because adaptations to the "never" therapy required marked upregulation of one driver gene, in particular gene 16 (Figure 6b). When applying solely the targeted therapy, only 9% of tumors were completely eradicated. Remarkably, if all tumors are first given the "never gene" upregulation therapy followed by the targeted therapy on gene 16, 80% of tumors were completely eradicated. This is an example of an evolutionary double bind therapy, where an initial therapy forces a precise evolutionary reaction, in this case an upregulation of gene 16, which is specifically treatable by the secondary therapy (19).

Methods

Fecundity and survivorship trade-off

We model carcinogenesis within the classic evolutionary life-history trade-off: fecundity versus survivorship (20–23). This trade-off becomes inevitable in any evolving population. As tumor cell populations grow and compete, cells can either increase life span through survival strategies that promote longevity at the cost of a reduced reproduction rate, or vice-versa. But, simultaneous increase in both is impossible (20–22).

A cell's fitness (per capita growth rate) is given as:

$$\omega(\mathrm{S},\mathrm{p})=\ln\left[2Sp+\frac{1}{2}(1-S)p+S(1-p)\right] \quad (1)$$

where *S* is the probability of surviving, and *p* as the probability of undergoing cell division. The term in brackets represent the finite growth rate of a cell based on its probability of dying and/or dividing in a given time step (often denoted as λ in models of population growth (24)), and the logarithm of the finite growth rate gives the instantaneous per cell growth rate

$$\frac{1}{x}\frac{\delta x}{\delta t}=\ln(\lambda) \quad (2)$$

where x is the population size of tumor cells. The formulation of this fitness function is described in Figure 7c. Note *S* and *p* combine several cancer "hallmarks" (5) as *p* is governed by self-sufficiency from growth signals and insensitivity to anti-growth signals and *S* represents evasion from apoptosis and replicative immortality.

Pre-malignant initial conditions

We chose three different starting values for *S* and *p* (Figure 7b). They simulate the effects of genetic and epigenetic variability in normal and pre-malignant cells due to random mutations, environmental factors, such as chronic inflammation, or germ line variations in different individuals. The initial values of *S* and *p* for these three initial conditions were set to just allow cells to replace individuals that are lost. This maintains a regulated, stable, and sustainable population of normal cells.

Genetic mutations

Normal cells evolve toward a malignant phenotype by stochastically accumulating mutations at any of 16 gene loci. We treat all gene mutations as haplotypes and permit just two haplotypes per locus: wild-type (state of normal cell) or mutated (not present in the normal cells). In the simulations, 22 genes were examined. Of these, 4 did not affect either fecundity or survivorship and served as neutral or passenger genes. 16 “active” (i.e. altered the cell fitness) genes each conferred a unique change in survival, S, and fecundity, *p* (Figure 7a), resulting in (2^{16}) 65,536 possible combinations of cumulative changes in *S* and *p* (Supplementary Figure 2), and 2 genes resulting in immediate cell death. The computer code used in the study and the raw data from simulations are available at https://github.com/cunninghamjj/Evolutionary-triage-in-Cancer. The location of the 16 genes in the fecundity and survivorship landscape were created using a randomizing algorithm under two rules; 1) 4 genes must lie in each quadrant and 2) the range for both fecundity and survivorship will fall between −0.2 and 0.2, which is the mean distance between the values of normal cells and the tumor ESS sites. As shown in Supplementary Figures 2 and 3, with these methods, 16 active genes were the minimum number sufficient to allow genetic access to cover the relevant evolutionary adaptive landscape. Fewer than 16 resulted in patchy inconsistent coverage and more than 16 showed diminishing returns of landscape coverage vs. computational requirement (Supplementary Figure 3). In multiple simulations we find that the locations of these 16 genes will affect the specifics of the results, such as which genes are “drivers” and which combine to create successful combinations. However, it does not affect the overall conclusions pertaining to heterogeneity.

In our simulations, 4 genes moved the cellular fitness toward higher values of both *S* and *p* and 4 other genes increase either just fecundity or just survivorship. These represent potential “drivers” in that they can increase fitness within the adaptive landscape. More genes could be added at the price of increased complexity and computational time. However, the simulation seemed consistent with recent analysis of genomic changes in different cancer types (25,26) that found 2 to 8 driver mutations in most tumors. The other genes either have no effect (i.e. classic passengers) or a negative effect on fitness.

Evolutionary stable strategies

In our model two maximal fitness [*S, p*] points on the [*S, p*] trade-off boundaries (Figure 1b) represent different adaptive landscapes due to, for example, regional variations of blood flow. The boundary is defined by the following equation:

$$p^{\alpha}+S^{\beta}=1 \quad (3)$$

We view one fitness maximum as a well-vascularized, nutrient rich area selecting for greater investment in proliferation (α=1, β=4) resulting in a ω(S,p) = 0.2996. While the second fitness maximum is an area of diminished blood flow selecting for greater investment in survival (α=3, β=6) resulting in ω(S,p) = 0.3005.. Evolution from one of the three initial conditions to one of the two maximal fitness points requires different evolutionary trajectories reflecting variations in selection pressures. These fitness maxima were not selected arbitrarily but represent the evolutionarily stable strategies (ESS of Maynard Smith (27)) that emerge from letting the tumor cells engage in an evolutionary game in which each cell's fitness-maximizing strategy depends upon the strategies of the other cells (28).

Two limits are imposed upon the evolving tumors: a carrying capacity and the fecundity versus survivorship trade-off. The former represents proliferation limitations due to restrictions in space and substrate and is simulated by randomly culling cells when the population exceeds its carrying capacity. The latter is imposed by the fitness landscape (Figure 7).

Mutation Rate

While simple, we favor this model for three reasons. First, it follows the pattern of reproduction used by cancer cells, which, as clonal propagators, lack meiosis and the Mendelian properties of segregation and independent assortment. Second, the altered genetics are not only a product of explicit mutations, but could also result from regulator genes, heritable epigenetic changes, other coding genes, and/or gene duplications and deletions. Third, while simplifying to two gene states at 16 loci offers many fewer "degrees of freedom" than the genome of a cancer cell, it is consistent with the number of driver genes typically observed in a wide range of cancers, and it allows us to follow explicit gene states. We recognize that reversal of each actual mutation is ordinarily viewed as improbable, but has been well documented in a wide range of organism traits (29). Furthermore, the reversal of the phenotypic consequence of most genetic changes can occur when the environmental selection forces change. A simple example is reversal of the MDR phenotype in-vitro when chemotherapy is removed from the culture media (30).

In the simulations presented here, we used a mutation probability of 0.01 per cell per division. When a mutation event occurred it was randomly assigned to one of the 16 genes. The actual mutation rate in cancer cells is not well established and hence a controversial topic. The estimated/measured number of mutations/cell/division varies widely. In fact, one motivation for this work was to examine variations between the actual underlying mutation rate and the observed mutation rate in each gene as a result of evolutionary triage. In our preliminary work (Figure 2), we found the results are unaffected by using mutation rates that were an order of magnitude lower or higher than 0.01. With a mutation rate above 10% the cell lineages cannot stay at the ESS due to wandering from a mutation-selection balance (31), while substantially lower mutation rates (10^{-4}) made evolution too slow for achieving the ESS even after 2000 generations.

The value is greater than that typically observed in normal cells (32) and in the general range of estimated cancer mutation rates other studies (33). Thus, the choice seemed biologically reasonable and, importantly, allowed computational efficiency without loss of general applicability.

Simulations and replications

We simulated cancer development during 1000 cell generations (representing 3 to 10 years depending on the rates of cell division) in "patients" under the 9 simulation permutations with 25 replicates for a total of 225 "patients". The 9 reflect the three starting phenotypes and three possible evolutionary trajectories (ESS1, ESS2, and transition from ESS1 to ESS2 due to temporal variations in blood flow) (Supplementary Figure 1).

Once tumors are established, we simulated targeted therapy by assuming that the resulting change in a driver gene renders the cell non-replicative and imposes a specific mortality rate of 25% per generation time. In addition, the dynamics of therapies targeted to "non-driver" genes and combinations of therapies can be analyzed. 900 simulated patients were analyzed for this model (data available at http://tinyurl.com/ntslsy8).

Discussion

Our goal in this work is to contribute to the development of a Darwinian theoretical framework for the large and often confusing molecular data sets generated by cancer biologists and oncologists. Recently, Weinberg, writing in a *Cell* commentary (34), observed that the common genetic paradigm of cancer "has reigned supreme for four decades" but he advocated a "move back to confronting the endless complexity of the disease." He concluded: "… it is becoming increasingly apparent that a precise and truly useful understanding of the behavior of individual cancer cells and the tumors that they form will only come once we are able to integrate and then distill these data". In a 2013 *Nature* article (35), we wrote: "Ultimately, real progress in understanding cancer biology will require a formal intellectual framework. Like gravity or quantum field theory in the physical sciences, we must define the underlying principles governing the nonlinear dynamics that give rise to the vast and complex data sets being generated by the creative minds of molecular biologists. These principles will not be found until we begin to search in the right place."

Here we examine Darwinian dynamics as the unifying first principles of cancer and use a classical evolutionary trade-off to clarify the molecular heterogeneity found in most cancers. The proposed evolutionary dynamics are not explicitly genetic. We focus on phenotypic interactions with environmental selection forces and view genetics as the "mechanism of inheritance." However we show that this approach is entirely compatible with molecular data and provides both organizing principles and novel insights.

Our results demonstrate that the extensive genetic data sets now available in cancer need to be understood in the context of "evolutionary triage" which governs the frequency with which any molecular property is *observed*. That is, following a random genetic or epigenetic change in a cancer cell, proliferation of the resulting phenotype is dependent on the fitness effect which is, in turn, governed by the prior genetic trajectory of the cell, local

environmental selection forces, and the extant populations. Thus, the distribution of observed mutations can be used to understand and simulate evolutionary and ecological dynamics within a tumor. Here we models based on the evolutionary triage principle to examine current concepts of driver and passenger mutations, the source of intratumoral molecular heterogeneity and the efficacy of targeted therapy.

Our simulations produce molecular heterogeneity within tumor populations that is similar to clinical observations. Our simulation demonstrate that this diversity is not an inevitable result of accumulating mutations but rather a consequence of variable selection forces due to environmental heterogeneity caused, for example, by variations in blood flow. In fact, our simulations find that, due to evolutionary triage, the diversity of tumor populations and the apparent mutation rate within a stable region will significantly *decline* after reaching a fitness maximum.

Our model also demonstrates that mutations that confer an increase in fitness will be observed with higher frequency than those that do not, consistent with the general bimodal classification of drivers and passengers. However, we find that accurate designation of driver or passenger mutation is possible only when the evolutionary and ecological context is known. That is, some mutations may be drivers in one environment but not another. This context dependence has been experimentally observed in the Wilms' tumor 1 (WT1) gene (18). Furthermore, the state of the cell along the genetic trajectory is critical so that a mutation can be a driver early in the evolutionary process but may not confer an equal adaptive advantage in later stage cells. In general, this demonstrates the principle of supervenience or functional equivalence (10, 30) in which cancer cells exhibit phenotypic convergence (i.e. the hallmarks) but through multiple different genetic trajectories resulting in genotype divergence.

Finally, our results demonstrate that therapy targeted to commonly observed mutations (regardless of their designation as driver or passenger) will generally reduce the population and occasionally produce a complete and prolonged response. However, uncommon extant populations that achieve maximal fitness through some other genetic trajectory are virtually always present and eventually permit tumor progression. This is consistent with results of targeted therapies in lung cancer and melanoma (31,32).

Perhaps the most non-intuitive prediction of the evolutionary triage model is that mutations that are never or rarely observed may provide a more consistent and durable response. This builds on prior results that used information theory to demonstrate changes in critical genes cannot be observed in a Darwinian environment (36). These mutations are, thus, eliminated by evolutionary triage because their normal function is necessary to maintain cancer cell fitness and thus both up and down regulation unconditionally results in a decrease in fitness. Interestingly, systematic investigation of knockout mutants in Escherichia coli found about 10% of genes were indispensable but this could vary considerably base on the culture conditions (37,38). This dependence on microenvironmental conditions is consistent with our general results that the fitness value of a gene (whether driver, passenger, or never) will depend on the critical selection forces within the environment, which can vary.

To further investigate this, we searched the Cancer Genome Atlas (TCGA) datasets for genes that are not listed. This demonstrated 1100 genes of 20,000 protein coding genes (5.5%) are not mutated in any of the TCGA datasets (total of ~ 4400 patients). The prediction that targeting never genes can be an effective therapy will require explicit investigation to confirm or refute. We do note, however, that while the proximal components of the MAPK pathway (EGFR, RAS, and RAF) are “driver” mutations, gain or loss of function mutations in the distal components, MEK and ERK are rarely observed. The obvious strategy is blocking a never gene and both MEK and ERK inhibitors are under investigation (39,40). However, a less obvious strategy is upregulating MEK expression. While this initially seems counter-intuitive, the simple observation that such a mutation is not observed in cancer suggests that over-expression of MEK also reduces fitness in a tumor environment (probably because unmodified proliferative signals will produce mitosis in inadequate environmental conditions leading to cell death). Our results suggest a counter-intuitive approach in which therapy that increase activity of MEK, ERK and other distal components of pathways may be a highly effective therapy. Finally, our model also suggest that combination therapies sequentially targeting a never mutations followed by targeting a compensating driver mutation may be substantially more effective than either treatment alone. Finally, we note that sequential therapy targeting first a never mutation followed by treatment of a classic driver phenotype had a high probability of eliminating the entire cancer population. This is because the tumor cells that were adapted to the first therapy universally required the driver mutation to maintain fitness – a therapeutic strategy classified as “double bind (41).”

Supplementary Material

Refer to Web version on PubMed Central for supplementary material.

Acknowledgments

This work is supported by the following National Institutes of Health/National Cancer Institute (NIH/NCI) grants: U54CA143970-01, and R01CA170595 and a grant from the James S. McDonnell Foundation. The authors thank Dr. Mohammad Fallahi-Sichani for his review of the TCGA data bases and Dr. John Cleveland for his insightful discussions and editorial suggestions.

References

1. Nowell PC. The clonal evolution of tumor cell populations. Science. 1976; 194:23–8. [PubMed: 959840]
2. Merlo LM, Pepper JW, Reid BJ, Maley CC. Cancer as an evolutionary and ecological process. Nature Rev Cancer. 2006; 812:924–35. [PubMed: 17109012]
3. Greaves M, Maley CC. Clonal evolution in cancer. Nature. 2012; 481:306–13. [PubMed: 22258609]
4. Komarova NL, Sengupta A, Nowak MA. Mutation-selection networks in cancer initiation: tumor suppressor genes and chromosomal instability. J Theor Biol. 2003; 223:433–50. [PubMed: 12875822]
5. Hanahan D, Weinberg RA. Hallmarks of cancer: the next generation. Cell. 2011; 144:646–674. [PubMed: 21376230]
6. Bozic I, Antal T, Ohtsuki H, Carter H, Kim D. Accumulation of driver and passenger mutations during tumor progression. Proc Natl Acad Sci USA. 2010; 107:18545– 18550. [PubMed: 20876136]

7. McFarland CD, Korolev KS, Kryukov GV, Sunyaev SR, Mirny LA. Impact of deleterious passenger mutations on cancer progression. Proc Natl Acad Sci USA. 2013; 110:2910–2915. [PubMed: 23388632]
8. Diaz LA, Williams RT, Wu J, Kinde I. The molecular evolution of acquired resistance to targeted EGFR blockade in colorectal cancer. Nature. 2012; 486:537–40. [PubMed: 22722843]
9. Crespi B, Summers K. Evolutionary biology of cancer. Trends Ecology and Evolution. 2005; 20:545–52. [PubMed: 16701433]
10. Gatenby RA, Gillies RJ. A microenvironmental model of carcinogenesis. Nat Rev Cancer. 2008; 8:56–61. [PubMed: 18059462]
11. Gerlinger M, Swanton C. How Darwinian models inform therapeutic failure initiated by clonal heterogeneity in cancer medicine. Br J Cancer. 2010; 103:1139–43. [PubMed: 20877357]
12. Wilkinson L. Systat Wiley Inter Reviews: computation statistics. 2010; 2:256–7.
13. Zhou M, Hall L, Goldgof D, Russo R, Balagurunathan Y, Gillies R, Gatenby R. Translational Oncology. 2014; 7:5–13. [PubMed: 24772202]
14. Stratton MR, Campbell PJ, Futreal PA. The cancer genome. Nature. 2009; 458:719–24. [PubMed: 19360079]
15. Jackson AL, Loeb LA. The mutation rate and cancer. Genetics. 1998; 148:1483–90. [PubMed: 9560368]
16. Gatenby RA, Gillies RJ, Brown JS. Of cancer and cave fish. 2011; 11:237–8.
17. Kudchadkar RR, Smalley KS, Glass LF, Trimble JS, Sondak VK. Targeted therapy in melanoma. Clin Dermatol. 2013; 31:200–8. [PubMed: 23438383]
18. Maemondo M, et al. Gefitinib or chemotherapy for non-small-cell lung cancer with mutated EGFR. New England J of Med. 2010; 362:2380–8. [PubMed: 20573926]
19. Cunningham JJ, Gatenby RA, Brown JS. Evolutionary dynamics in cancer therapy. Mol Pharm. 2011; 8:2094–2100. [PubMed: 21815657]
20. Stearns SC. Trade-offs in life-history evolution. Functional Ecology. 1989; 3:259–268.
21. Atkipis A, Boddy AM, Gatenby RA, Brown JS, Maley CC. Life history trade-offs in cancer evolution. Nature Rev Cancer. 2013; 13:883–92. [PubMed: 24213474]
22. Mukhopadhvav A, Tissenbaum HA. Reproduction and longevity: secrets revealed by C. Elegans. Trends Cell Biol. 2007; 17:65–71. [PubMed: 17187981]
23. Marden JH, Rogina B, Montooth KL, Helfand SL. Conditional tradeoffs between aging and organismal performance of Indy long-lived mutant flies. Proc Natl Acad Sci USA. 2003; 18:3369–73. [PubMed: 12626742]
24. Case, TJ. An illustrated guide to theoretical ecology. Oxford Press; 2001.
25. Kandoth C, et al. Mutational landscape and significance across 12 major cancer types. Nature. 2013; 502:333–9. [PubMed: 24132290]
26. Yang L, Han Y, Suarez Saiz F, Minden MD. A tumor suppressor and oncogene: the WT1 story. Leukemia. 2007; 21:868–876. [PubMed: 17361230]
27. Smith MJ, Price GR. The logic of animal conflict. Nature. 1973; 246:15–18.
28. Pintor LM, Brown JS, Vincent TL. Evolutionary game theory as a framework for studying biological invasions. Am Nat. 2011; 177:410–23. [PubMed: 21460564]
29. Muller HJ. Reversibility in evolution considered from the standpoint of genetics. Biological Rev. 1939; 14:261–280.
30. Bellamy WT, Dalton WS. Multidrug resistance in the laboratory and clinic. Adv Clin Chem. 1994; 31:1–61. [PubMed: 7879670]
31. Haldane JBS. A mathematical theory of natural and artificial selection, Part V: selection and mutation. Math Proc of the Cambridge Philosph Soc. 1927; 23:838–844.
32. Roach JC, et al. Analysis of genetic inheritance in a family quartet of whole-genome sequencing. Science. 2010; 328:636–9. [PubMed: 20220176]
33. Loeb LA. A mutator phenotype in cancer. Cancer Res. 2001; 61:3230–9. [PubMed: 11309271]
34. Weinberg R. Coming full circle – from endless complexity to simplicity and back again. Cell. 2014; 157:267–271. [PubMed: 24679541]

35. Gatenby R. Finding cancer's first principles. Nature. 2012; 491:55.
36. Gatenby RA, Frieden BR. Application of information theory and extreme physical information to carcinogenesis. Cancer Res. 2002; 62:3675–84. [PubMed: 12097274]
37. Tohsato Y, Baba T, Mazaki Y, Ito M, Wanner BL, Mori H. Environmental dependency of gene knockouts on phenotype microarray analysis in Escherichia coli. J Bioinform Comput Biol. 2010; 1:83–99. [PubMed: 21155021]
38. Joyce AR, et al. Experimental and computational assessment of conditionally essential genes in Escherichia coli. J Bacteriol. 2006; 188:8259–71. [PubMed: 17012394]
39. Salama AK, Kim KB. The evolution of melanoma resistance reveals therapeutic opportunities. Cancer Res. 2013; 73:6106–10. [PubMed: 24097822]
40. Wong DJ, et al. Antitumor activity of the ERK inhibitor SCH722984 against BRAF mutant, NRAS mutant and wild-type melanoma. Mol Cancer. 2014; 13:194–201. [PubMed: 25142146]
41. Gatenby RA, Brown J, Vincent T. Lessons from applied ecology: cancer control using an evolutionary double bind. Cancer Res. 2009; 59:7499–502. [PubMed: 19752088]

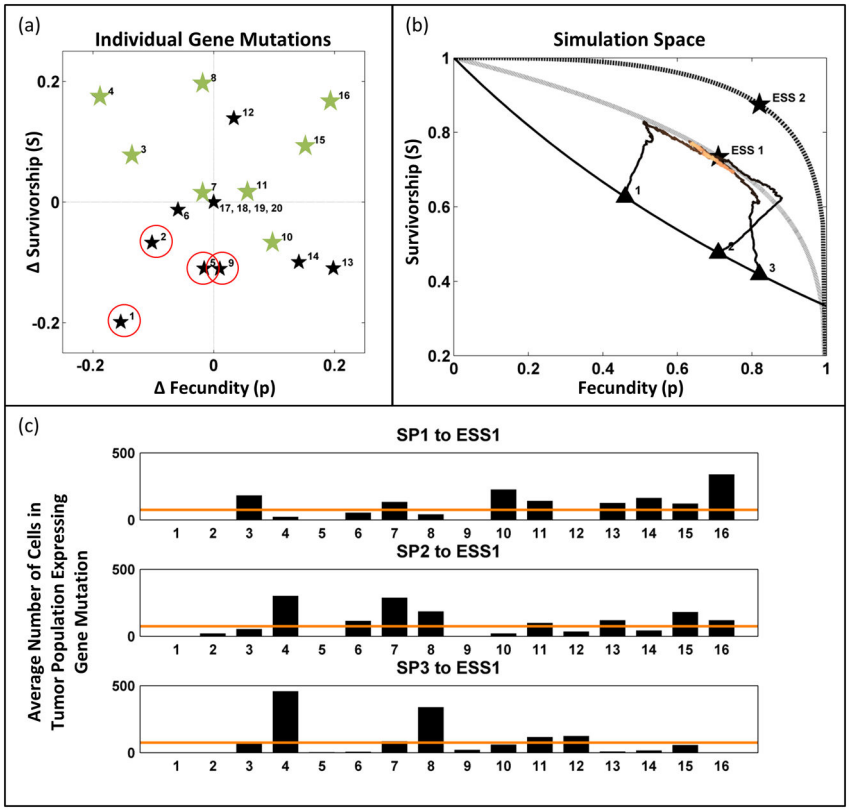

Figure 1.

Evolutionary Trajectories and Gene Prevalence. a) During evolution to ESS1 (Evolutionary Stable State 1), the genes highlighted in green conferred increased fitness depending on starting initial phenotype. The genes circled in red, such as gene 1, reduce both fecundity and survivorship and were never observed in the final simulated cancer populations. b) Multiple evolutionary trajectories exist to ESS1 depending on initial phenotype. This functional equivalence results in genetic heterogeneity within and between patients as seen in c. c) The mutation prevalence varies greatly depending on initial phenotype. The orange line represents the neutral mutation prevalence.

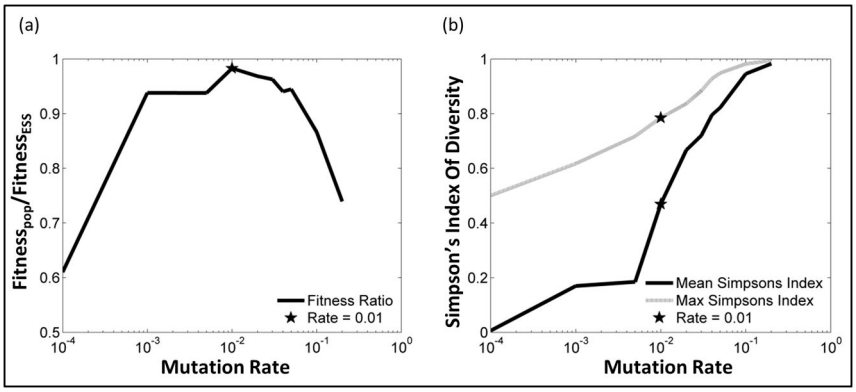

Figure 2. Effect of Different Mutation Rates

(a) The y-axis shows the ratio between the mean fitness reached by the population after 2000 generations and the fitness achievable at the ESS (See Figure 2b). For this example we used ESS 1 with a maximum fitness = 0.3). The x-axis varies the mutation rate with units of mutation/cell/division with the lowest value slightly higher than that of normal cells (24). With a low mutation rate the evolution is too slow to reach the ESS. As the mutation rate increases (between 10^{-3} and 10^{-1}), the tumor population evolves to the ESS. However, at very high mutation rates, the population is unstable and fitness decreases due to a mutation/selection balance – a phenomenon predicted by Haldane (23). In (b) we demonstrate that the diversity of tumor populations increases with mutation rate. For the remaining simulations we chose a mutation rate of 10^{-2} (star) as the midpoint between these trade-offs.

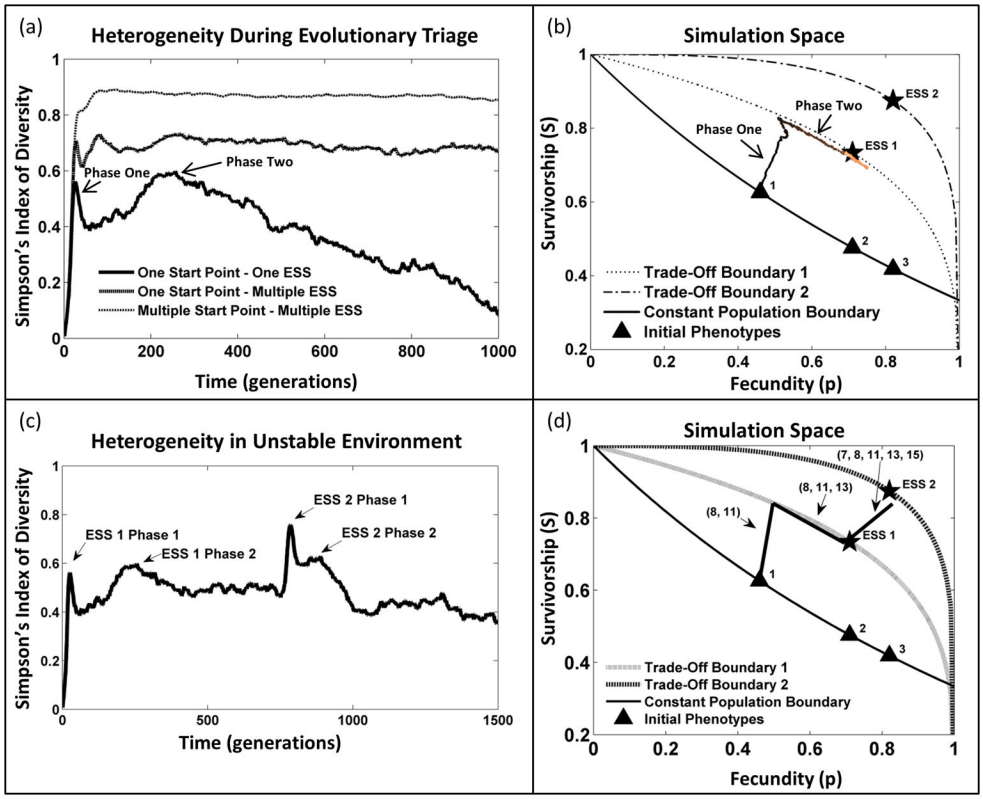

Figure 3. Simpson's Index of Diversity

We demonstrate that heterogeneity of intratumoral phenotypes will vary as tumor populations evolve along the adaptive landscape. In Panel (a) the Simpson's Index of Diversity is shown for stable or spatially varying landscapes. The solid line marked corresponds to the trajectory in Panel (b) in which there is a single, stable ESS. Initial somatic evolution results in a rapid increase in heterogeneity as the early tumor moves toward the trade-off boundary. However, during later evolution, the intratumoral populations decrease in heterogeneity as the tumor moves closer and closer to the maximal fitness point, ESS1. This predicts that tumor cells in a stable environment will exhibit on limited diversity. In contrast, for spatially complicated landscapes (Panels (c) and (d)) due, for example, to temporal and spatial variations in blood flow, heterogeneity remains high (Panel c). The results suggest that the observed heterogeneity in tumor largely reflects variations in environmental selection forces (i.e. vascular density and blood flow). Similar temporal variations during tumor development were predicted in Reference (2).

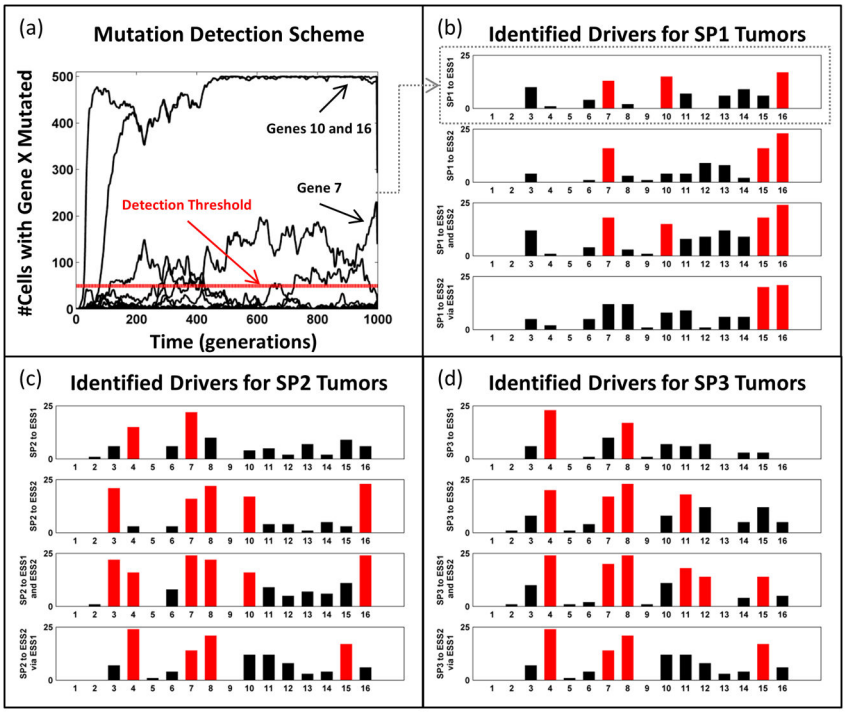

Figure 4. Identifying Driver Mutations

a) The gene mutation prevalence for one patient (initial phenotype 1 to ESS1) is shown. The "biopsy" occurs at the end of simulation, at 1000 generations. We assume that if at least 10% of the cells in the whole tumor exhibit a mutation in a particular gene at the time of biopsy, it will be detected. In this particular biopsy, mutations in genes 7, 10, and 16 would be identified. b–d) This biopsy detection scheme is conducted for all patient samples and each detection is tallied. If a mutation in a particular gene is detected in at least 12 of the patients, it is highlighted in red.

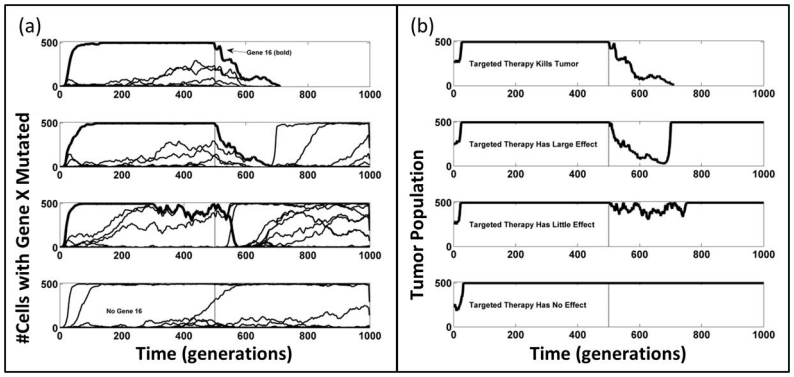

Figure 5. Mutation Prevalence and Population Dynamics of Tumors from Initial Phenotype 1 During Targeted Therapy Simulation

The underlying mutational prevalence for four representative tumors are shown in panel a while the corresponding population dynamics are shown in b. At the time of treatment (generation 500) the prevalence of mutation 16 drops to zero. After treatment, if the tumor survives, the evolutionary strategies used to reach maximal fitness can be observed. The top example shows the dynamics in 9.3% of patients where a full response to therapy is observed. The second shows a representative moderate response with eventual proliferation of resistant populations. The third shows a delay in progression though no significant response. The last example shows how in 28% of patients, the therapy had no effect.

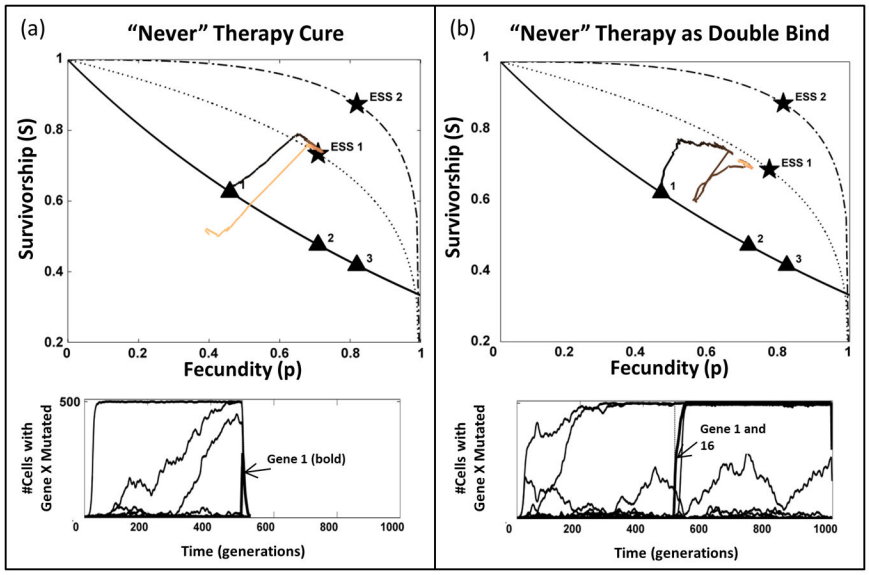

Figure 6. "Never" Therapy Outcomes

a) On the left, the evolutionary trajectory to ESS1 from initial phenotype 1 is shown in black. After the "never" therapy is administered the trajectory falls below the sustainability line and results in tumor extinction, shown in orange. More commonly the "never" therapy does not cause tumor eradication but because cells with mutated gene 16 survive and remain sufficiently fit to proliferate and repopulate the tumor b). This represents a classical treatment "double bind' (41) and renders the tumor exceedingly susceptible to the traditional targeted therapy directed against driver gene 16. In 80% of simulations, this strategy produced complete tumor eradication.

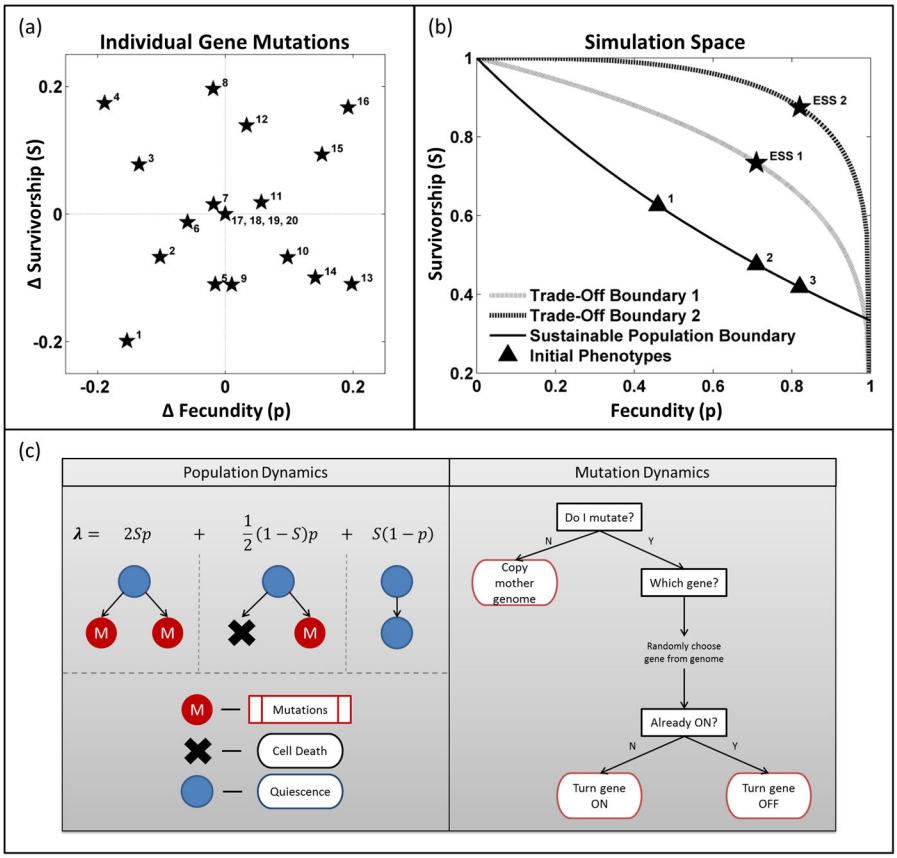

Figure 7. Simulation Setup

a) Each of the 16 mutations confers a unique change to fecundity and survivorship. For example, mutation 16 increases both fecundity and survivorship a large and equal amount while mutation 9 greatly decreases survivorship but has no effect on fecundity. Mutations 17–20 true passenger mutations, conferring no change in survivorship or fecundity. b) Normal cells are found on the solid line, with the three specific normal populations used in the simulations highlighted (triangles). When carcinogenesis is allowed cells evolve from their original phenotype toward the dotted lines which represents the trade-off between survivorship and fecundity above which cells require too many resources, and are unable to survive. The point at which the fitness of an evolving cell within the extant environment is maximized is highlighted (stars). The path from a starting point to the maximization point corresponds to somatic evolution during carcinogenesis and represents acquisition of the hallmarks of cancer outlined in the text. c) Our fitness formulation assumes three distinct cell outcomes for each generation. 1) A cell can divide, allowing mutations in both mother and daughter, 2) a cell can survive first and then may divide (death precedes cell division), or divide first and then the progenitor cell may die (cell division precedes death), and 3) a cell may continue to the next generation. The mutation dynamics outline the process by which a mutation event is determined.